scientific reports

Check for updates

OPEN

Development of a bioassay-guided genome mining approach for antifungal natural product discovery from pseudomonads

George Lund[1]✉, Susan Mosquito[1], David M Withall[1], John Caulfield[1], David Hughes[1], Ian M Clark[2], Jason Rudd[1] & Tim H Mauchline[1]

Zymoseptoria tritici **causes Septoria Leaf Blotch disease of wheat and has evolved to overcome most chemical and genetic control methods. As such, new tools are required for future disease control. We identified *Pseudomonas* isolates that antagonise *Z. tritici* through the production of secreted secondary metabolites, using a novel in vitro antagonism assay. Quantitative assessment identified variation in sensitivity of *Z. tritici* isolates to antagonism by *Pseudomonas* isolates. Genome assemblies of 3 strongly antagonistic *Pseudomonas* isolates contain a predicted Biosynthetic Gene Cluster (BGC) with high similarity to a reference BGC encoding the biosynthesis of known antifungal compound 2,4-diacetylphloroglucinol (2,4-DAPG). Mutagenesis of the core biosynthetic gene *phlD* resulted in loss of 2,4-DAPG production in *Pseudomonas* isolate Roth82, and loss of *Z. tritici* inhibition in vitro. These results demonstrate that our in vitro antagonism assay can be used to identify, quantify, and mechanistically characterise bacterial antagonism of *Z. tritici* through the production of secondary metabolites. This is the first study to putatively identify that resistance to bacterial antagonism exists as a quantitative trait within natural *Z. tritici* populations. Our approach of in vitro phenotype-guided genome mining can also prioritise candidate BGCs for discovery of antifungal natural products effective against *Z. tritici*.**

Keywords Secondary metabolites, *Zymoseptoria tritici*, *Pseudomonas*, Antagonism, Bacterial-fungal interactions, Bioassay

Wheat is the UK's most widely grown crop, but yield is diminished due to diseases caused by pathogenic fungi. The most important disease of wheat in the UK is Septoria tritici blotch, caused by the fungus *Zymoseptoria tritici*, resulting in up to 50% yield losses[1]. Wheat has no durable natural resistance and the fungus has become insensitive to all classes of existing commercial fungicides[2]. Therefore, new ways to protect wheat are urgently needed. One underexplored approach is to exploit natural antifungal chemistries encoded within microbial genomes.

The soil microbiome is diverse and largely untapped for the discovery of new molecules that can suppress plant pathogens. To date, most antimicrobial compounds have been derived from soilborne actinomycetes[3]. *Pseudomonas* bacteria are an important component of the soil microbiome with exemplar species behaving as human pathogens[4](e.g. *P. aeruginosa*), plant pathogens[5](e.g. *P. syringae*), as well as plant growth promoting bacteria[6], and biocontrol agents[7,8](e.g. *P. fluorescens*); yet the diverse secondary metabolite repertoire of this genus, which has potential for the discovery of new high value fungicides, is relatively underexplored experimentally[9].

Previous studies investigating in vitro antagonism of *Z. tritici* by *Pseudomonas aeruginosa* isolate LEC1, found the siderophore pyocyanin[10] and 1-hydroxyphenazine[11,12] to partially contribute towards antagonism. *Pseudomonas fluorescens* PMF2 was found to antagonise *Z. tritici* through the production of 2,4-diacetylphloroglucinol (2,4-DAPG) and 2 additional unidentified antifungal compounds (Levy et al.,[13]. Tropolone, produced by *Pseudomonas lindbergii*, was found to inhibit the growth of *Z. tritici* in vitro[14,15]. *Pseudomonas* isolates have also previously been shown to antagonise *Z. tritici* through the production of volatile compounds, with *Pseudomonas putida* BK8661 found to antagonise *Z. tritici* through the production of hydrogen

[1]Translating Biotic Interactions, Rothamsted Research, West Common, Harpenden AL5 2JQ, Hertfordshire, UK. [2]Soil Health and Management, Rothamsted Research, West Common, Harpenden AL5 2JQ, Hertfordshire, UK. ✉email: george.lund@rothamsted.ac.uk

cyanide (HCN) in vitro[16]. In vitro studies investigating the antagonistic potential of bacterial isolates against fungal plant pathogens, have mostly consisted of single genotypes of fungal plant pathogens[16,10,13,12,14]. However, *Z. tritici* has high levels of genetic diversity, with previous studies identifying over 600 different genotypes of the fungus in a single field over a single season[17], and individual leaf lesions were found to harbour 2–5 different genotypes[18].

Quantification of in vitro antagonism of fungal pathogens by bacterial isolates is difficult, owing to the filamentous hyphal growth of many fungal pathogens, and therefore measurements have commonly taken place through qualitative assessments[19,20]. Quantitative assessment of in vitro *Z. tritici* antagonism could facilitate the identification of *Pseudomonas* isolates capable of antagonising *Z. tritici* in vitro in a broader context. Such assessments could facilitate sensitivity comparisons of genetically diverse *Z. tritici* isolates to antagonistic *Pseudomonas* isolates. Pseudomonads are generally amenable to culture and this property facilitates the acquisition of their genomes, which in turn assists in the identification of the genetic components responsible for the biosynthesis of antifungal or fungistatic secondary metabolites[21].

This study introduces a novel qualitative and quantitative blastospore-based assay for high throughput assessment of pseudomonad growth suppression of multiple *Z. tritici* genotypes. The radial zones of clearing produced by antagonistic *Pseudomonas* isolates, confronted with *Z. tritici* blastospores as a confluent lawn, offer the potential to both qualitatively and quantitatively assess antagonism of *Z. tritici* by *Pseudomonas* isolates. This assay in combination with genomics, microbial mutagenesis and analytical chemistry enables the prioritisation of predicted secondary metabolite Biosynthetic Gene Clusters (BGCs) from antagonistic isolates for further characterisation, and comparison with BGCs previously described in literature from the MIBiG 3.0 repository[22]. We report the initial screening of a *Pseudomonas* library of 534 isolates for suppression of the *Z. tritici* reference isolate IPO323. Subsequent in vitro testing of 5 antagonistic and 6 non-antagonistic *Pseudomonas* isolates confronted with 12 genetically diverse *Z. tritici* isolates, revealed significant differences in resistance to bacterial antagonism. To our knowledge this is the first study to find evidence suggesting sensitivity to bacterial antagonism exists as a quantitative trait within natural *Z. tritici* populations. We demonstrate the power of a bioassay-mediated genomics approach to define potential antifungal secondary metabolite BGCs involved in bacterial-fungal interactions in vitro. The study also demonstrates the importance of testing genetically diverse individuals from within pathogen populations to ensure consistency of antagonistic responses ahead of further exploitation of bacterial secondary metabolites or biological control agents as future disease control strategies.

Results

Qualitative screening of *Z. tritici* IPO323 antagonism

A total of 534 *Pseudomonas* isolates were screened qualitatively for antagonism of *Z. tritici* IPO323 blastospores, with 52 identified as being antagonistic (Fig. 1, Table S1).

Pseudomonas isolates demonstrate variable quantitative suppression of a genetically diverse *Z. tritici* collection

Of the 52 *Pseudomonas* isolates that demonstrated qualitative antagonism to *Z. tritici* IPO323 blastospores, 5 antagonistic isolates alongside 6 non-antagonistic isolates (Table S2) from the collection were randomly selected and screened quantitatively for antagonism against a collection of 12 genetically diverse *Z. tritici* isolates collected from across Europe in 2015/16[23](Fig. 2). All 5 qualitatively antagonistic *Pseudomonas* isolates were found to suppress growth of *Z. tritici* IPO323 as well as the additional 11 genetically diverse *Z. tritici* isolates in the quantitative antagonism assay (Fig. 2). In addition, all 6 *Pseudomonas* isolates which had been determined

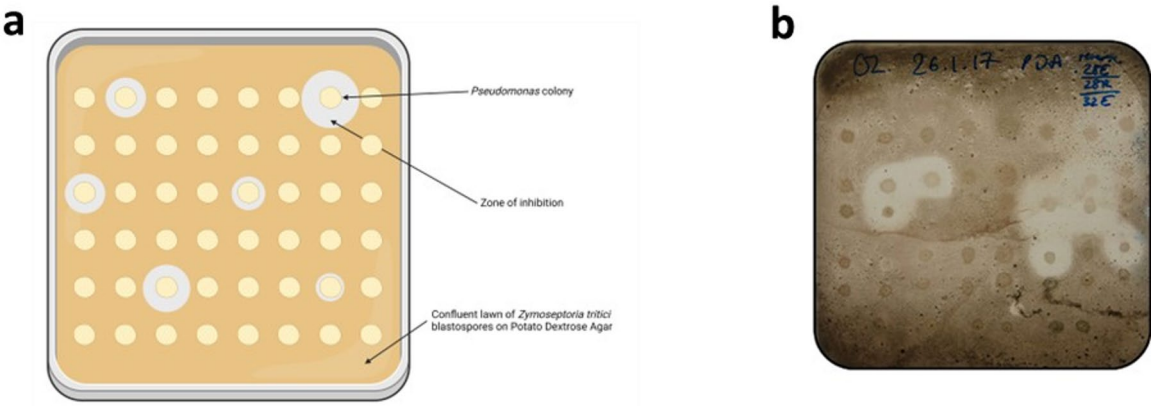

Fig. 1. A high-throughput qualitative assay to assess the ability of *Pseudomonas* antagonism of *Z. tritici* blastospores in vitro. **(a)** Schematic diagram of the qualitative *Z. tritici* blastopore antagonism assay. In the bioassay, *Pseudomonas* isolates are spotted onto a confluent lawn of *Z. tritici* blastospores on PDA. Created in BioRender. Lund, G. (2024) BioRender.com/p07z107 **(b)** A photograph of the qualitative *Z. tritici* blastospore antagonism assay, with 48 *Pseudomonas* colonies on one assay plate in confrontation with a single fungal isolate.

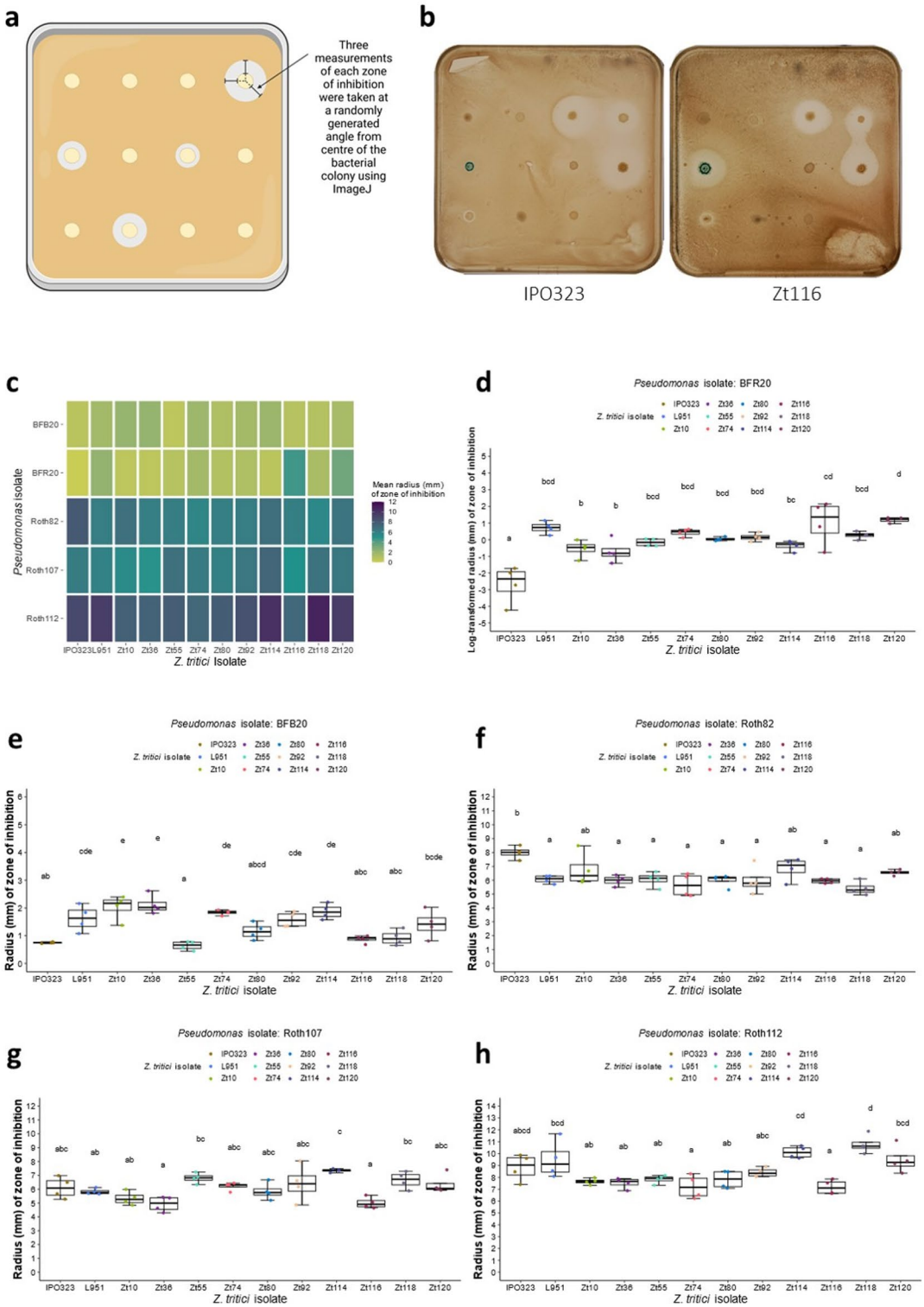

Fig. 2. Significant differences in zones of inhibition of genetically distinct *Z. tritici* blastospores by *Pseudomonas* isolates in vitro, using a quantitative antagonism assay. **(a)** A schematic diagram of the quantitative *Z. tritici* blastopore antagonism assay. Created in BioRender. Lund, G. (2023) BioRender.com/y78z760 **(b)** Images of in vitro quantitative antagonism plates exhibiting differences in zones of inhibition produced by *Pseudomonas* isolates against IPO323 and Zt116 blastospores. **(c)** Heatmap indicating the average radius of the zone of inhibition produced in each pairwise interaction between antagonistic *Pseudomonas* and *Z. tritici* isolates in the quantitative antagonism assay after 12 days ($n = 4$). **(d-h)** Zones of inhibition produced by *Pseudomonas* isolates in confrontation with genetically diverse *Z. tritici* blastospores in vitro. Mean values of zones of inhibition not sharing any letter are significantly different by Sidak's test for multiple comparisons at the 5% level of significance for *Pseudomonas* isolates **(d)** BFR20 **(e)** BFB20 **(f)** Roth82 **(g)** Roth107 **(h)** Roth112.

to be qualitatively non-antagonistic towards *Z. tritici* IPO323, as well as LB Miller Broth medium controls, did not produce an observable zone of clearing when confronted with any of the *Z. tritici* isolates screened (Figure S7). This indicates that IPO323 confrontation is an appropriate starting test for the identification of *Pseudomonas* isolates with the potential to antagonise *Z. tritici* isolates qualitatively in vitro.

A statistically significant difference in the mean zones of inhibition (millimetres) was detected between genetically diverse *Z. tritici* isolates confronted with antagonistic *Pseudomonas* isolates; BFR20 ($F(11, 36) = 11.48$, $p < 0.001$), BFB20 ($F(11, 36) = 10.97$, $p < 0.001$), Roth82 ($F(11, 36) = 4.455$, $p < 0.001$), Roth107 ($F(11, 36) = 5.567$, $p < 0.001$), and Roth112 ($F(11, 36) = 8.11$, $p < 0.001$). Significant differences in the mean zones of inhibition produced by antagonistic *Pseudomonas* were determined using Sidak's multiple comparison post hoc test (Fig. 2d-h, Tables S4-S13).

Genome sequencing, taxonomic estimation, and predictive bioinformatics of secondary metabolism of environmental *Pseudomonas* isolates

Genome assemblies were generated by MicrobesNG for the 11 *Pseudomonas* isolates examined in the quantitative *Z. tritici* antagonism assay. All genome assemblies were found to have BUSCO scores > 99%, when analysed using the bacterial odb10 dataset (containing 124 single copy orthologous genes) to check for bacterial contamination within the genome assembly (Figure S1). Additionally, BUSCO analysis of the generated genome assemblies using the Pseudomonadales odb10 dataset (containing 782 single copy orthologous genes) also returned BUSCO scores > 99% for all assemblies. BUSCO analyses indicated high levels of genome assembly completeness and low levels of genome assembly contamination (Figure S2).

To predict putative secondary metabolite biosynthetic gene clusters from the *Pseudomonas* genome assemblies, antiSMASH 7.0.0[24] was used. A total of 131 BGCs were predicted from the genome assemblies of the 11 *Pseudomonas* isolates (Figure S3). To compare predicted BGCs between *Pseudomonas* isolates, and compare to reference BGCs from the MIBiG 3.0 database[22], sequence similarity networks of predicted secondary metabolite BGCs from both antagonistic and non-antagonistic *Pseudomonas* isolates were generated using BiG-SCAPE[25], including reference BGCs from MIBiG 3.0. A total of 46 GCF networks were formed of two or more BGCs, with 3 GCFs containing a reference BGC from MIBiG 3.0 (GCF_00413, GCF_02527, GCF_02551, Fig. 3a), indicating similarity of predicted BGCs from *Pseudomonas* genome assemblies within this study, at the 0.3 threshold in BiG-SCAPE. A total of 13 GCF networks were found to contain predicted BGCs from solely *Z. tritici* blastospore antagonistic *Pseudomonas* isolates (Fig. 3a). Of these, GCF_02551 contained reference BGCs from MIBiG 3.0, BGC0000280 and BGC0000281, which have been shown experimentally to encode the biosynthesis of 2,4-diacetylphloroglucinol[26], a known antifungal compound effective at inhibiting *Z. tritici* in vitro(Levy et al.,[13]. Predicted BGCs within GCF_02551 were aligned using clinker, with high levels of amino acid similarity, and synteny identified between the reference BGCs and those predicted from the generated *Pseudomonas* genome assemblies (Fig. 3b).

To estimate the taxonomy of the generated *Pseudomonas* genome assemblies, autoMLST[27] was used. A phylogenetic tree was constructed using 100 common genes (Table S3) from the 11 *Pseudomonas* genome assemblies, with the closest 50 genome assemblies from RefSeq included in the phylogenetic tree construction. The closest RefSeq type strains to the genome assemblies generated in this study were cross referenced with previous literature to identify clades associated with described subgroups of the *P. fluorescens* species complex[28,29](Fig. 4).

Phylogenetic analysis indicated that the 11 *Pseudomonas* strains within this study span 4 distinct subgroups of the *P. fluorescens* species complex, as defined by Hesse et al.,[28]. Isolates predicted within the *P. corrugata* subgroup, Roth82, Roth107 and Roth112, were all found to exhibit antagonistic phenotypes when confronted with *Z. tritici* blastopores in vitro. Both *Z. tritici* blastospore antagonistic (BF-R-20) and non-antagonistic (A-B-20, Roth105) *Pseudomonas* isolates were found within the *P. mandelii* subgroup. Isolates Roth17 and Roth40, within the *P. fluorescens* subgroup, and Roth79 and Roth97 within the *P. jessenii* subgroup were all found to exhibit a non-antagonistic phenotype when confronted with *Z. tritici* blastospores in vitro.

The resulting phylogenetic tree was annotated with the GCF network data generated using BiG-SCAPE, to visualise the distribution of predicted BGCs with a high similarity to MIBiG reference BGCs (Fig. 4), and all predicted BGCs forming GCF networks (Figure S5). All 3 isolates classified within the *P. corrugata* subgroup (Roth82, Roth107 and Roth112) were found to contain predicted BGCs that formed a sequence similarity network with MIBiG reference BGCs encoding the production of 2,4-DAPG. The genome assemblies of *Z. tritici* non-antagonistic *P. fluorescens* subgroup isolates Roth17 and Roth40 were found to contain predicted BGCs with significant similarity to the MIBiG reference BGC encoding the biosynthesis of pseudomonine. Predicted BGCs with a significant similarity to MIBiG reference BGC BGC0000413, encoding the production of pyoverdine, were found in genome assemblies of the non-antagonistic *P. fluorescens* subgroup (Roth17 & Roth40), *P. jessenii* subgroup (Roth97), and *P. mandelii* subgroup (Roth105), as well as the antagonistic *P. mandelii* subgroup (BF-R-20) isolate.

Gene disruption of BGC predicted to encode the biosynthesis of 2,4-DAPG results in a loss of visible *Zymoseptoria tritici* antagonism, and a reduction in 2,4-DAPG detected in agar extracts of confrontation zones

Roth82 was selected for proof-of-concept functional validation because it was readily transformable under our conditions and carried a predicted 2,4-DAPG biosynthetic gene cluster with high similarity to reference clusters. To examine the involvement of known antifungal secondary metabolite 2,4-DAPG in the observed *Z. tritici* blastospore antagonism by isolate Roth82 (*P. corrugata* subgroup), a single *phlD* insertional mutant was constructed by insertional disruption using the pKNOCK-Km suicide vector as a proof of concept, in which the *phlD* gene was disrupted in Roth82, resulting in Roth82 *phlD*::pKNOCK-Km (Figure S6). *Zymoseptoria tritici* blastospore confrontation assays were undertaken with strain IPO323, with methanol agar extracts from

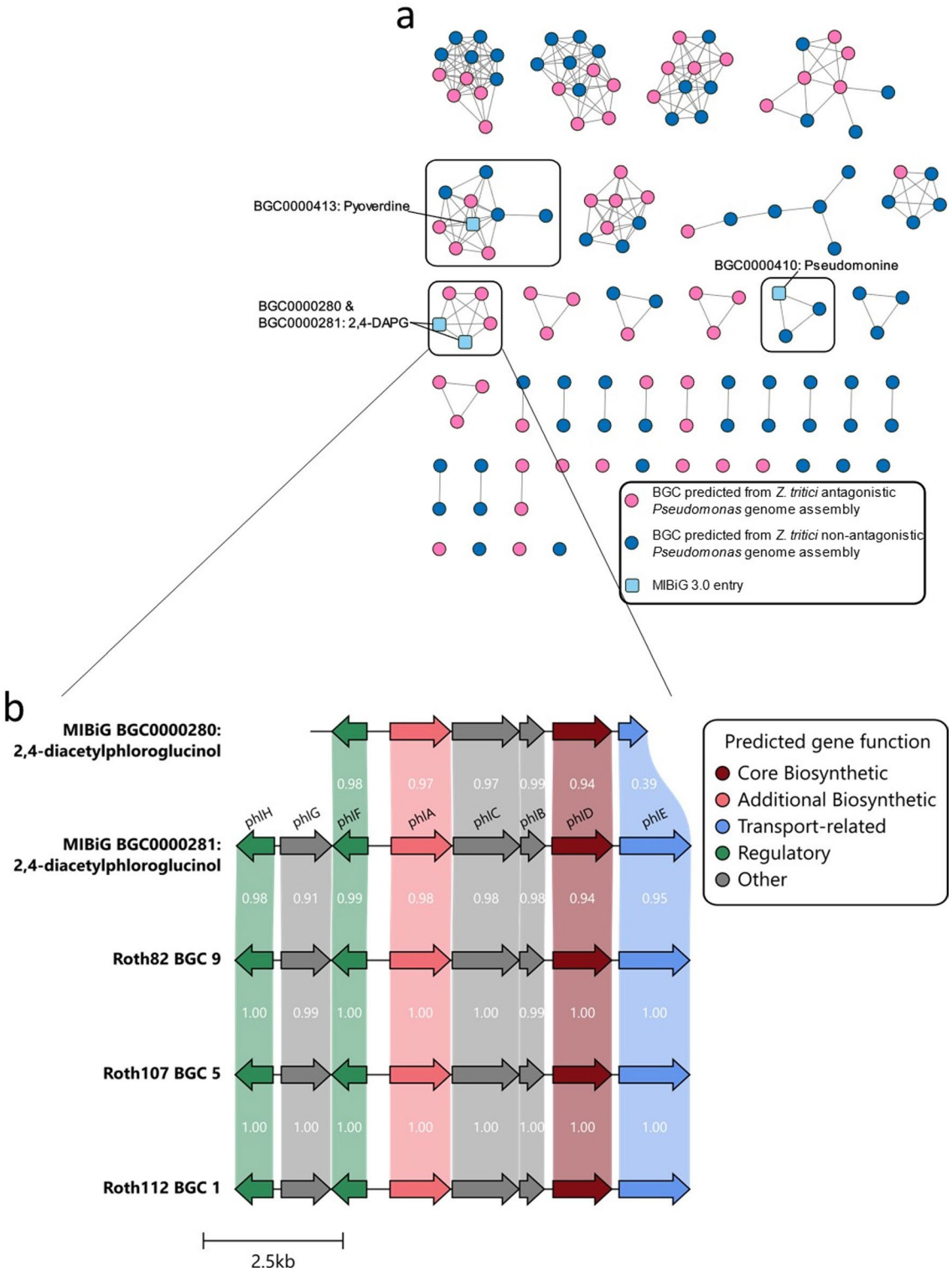

Fig. 3. Sequence similarity networks generated using BiG-SCAPE reveal Gene Cluster Families associated with the *Z. tritici* blastospore antagonism phenotype, including reference BGCs with known antifungal activity from the MIBiG repository. **(a)** Sequence similarity networks indicated predicted BGCs with high sequence similarity to MIBiG reference BGCs for pyoverdine (BGC0000413, GCF_02527), 2,4-DAPG (BGC0000280 & BGC0000281, GCF_02551), and pseudomonine (BGC0000410, GCF_00413), within the *Pseudomonas* genome assemblies. **(b)** Amino acid alignment of BGCs forming GCF_02551 with 2,4-DAPG biosynthesis reference BGCs from MIBiG (BGC0000280 & BGC0000281) indicates high levels of amino acid similarity and gene synteny between predicted BGCs.

Fig. 4. Phylogenetic distribution of *Pseudomonas* isolates with predicted secondary metabolite BGCs with significant similarity to known BGCs in relation to *Z. tritici* blastopore antagonism phenotypes. Phylogenetic analysis with known *Pseudomonas* strains, using autoMLST, putatively identifies 11 *Pseudomonas* strains used within this study within the *P. fluorescens*, *P. corrugata*, *P. koreensis*, *P. jessenii*, and *P. mandelii* subgroups of the *P. fluorescens* species complex. The presence and absence of predicted BGCs that form sequence similarity networks with experimentally characterised BGCs from the MIBiG database are indicated, alongside qualitative *Z. tritici* blastospore antagonism phenotype against *Z. tritici* strain IPO323. Type strain *Pseudomonas* genomes identified according to LPSN (accessed 24th January 2025) are denoted by a superscript 'T'.

the zone surrounding Roth82 and Roth82 *phlD*::pKNOCK-Km prepared after 12 days of confrontation. No visible zone of inhibition was present for Roth82 *phlD*::pKNOCK-Km (Fig. 5b), whereas a zone of inhibition was seen for wild-type Roth82 (Fig. 5a). These observed phenotypes correlated with LC-MS analysis of the agar extracts, with wild-type Roth82 extract showing a peak at m/z 209.0455 ± 5ppm $[M\text{-}H]^-$ with a retention time of 26.65 min (Fig. 5c), corresponding to the authentic chemical standard for 2,4-DAPG (Sigma, Fig. 5c). For

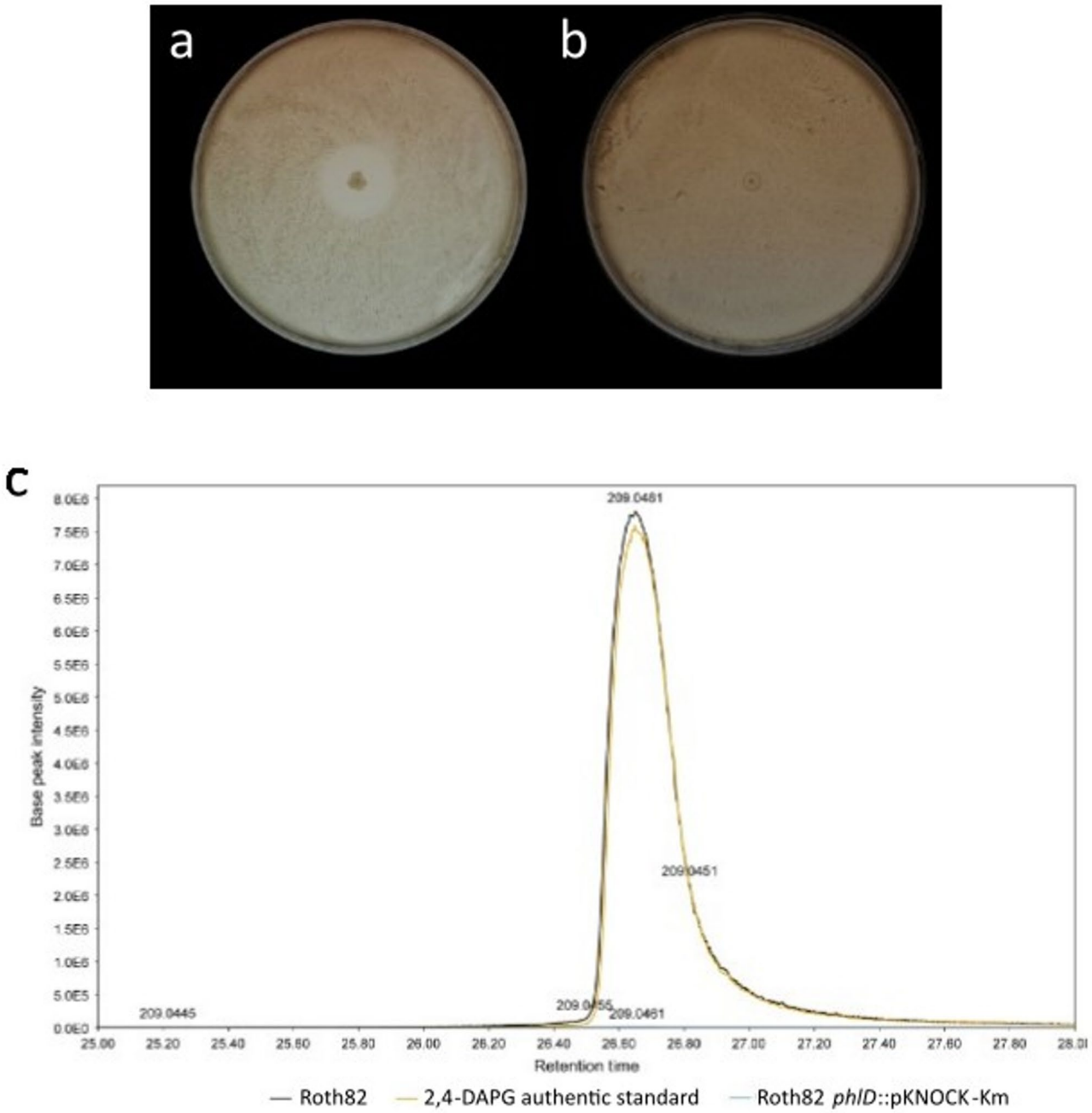

Fig. 5. Disruption of *phlD* in isolate Roth82 (*P. corrugata* subgroup) results in a loss of *Z. tritici* blastospore antagonism in vitro, and reduction in the production of 2,4-DAPG. *Zymoseptoria tritici* IPO323 blastospore antagonism assay with wild-type Roth82 exhibiting a zone of inhibition **(a)** and Roth82 *phlD*::pKNOCK-Km showing no zone of inhibition **(b)**. **(c)** Extracted ion chromatogram at m/z = 209.0455 with a mass tolerance of ± 5ppm, corresponding to $[M-H]^-$ (molecular formula $C_{10}H_9O_5$) of 2,4-DAPG ($C_{10}H_{10}O_5$). Liquid Chromatography-Mass Spectrometry analysis was performed on agar extracts from the area surrounding the colony of wild-type Roth82 in confrontation with *Z. tritici* IPO323 blastospores (black), Roth82 *phlD*::pKNOCK-Km in confrontation with *Z. tritici* IPO323 blastospores (turquoise), and the authentic chemical standard for 2,4-DAPG (Sigma, orange).

the Roth82 phlD::pKNOCK-Km mutant confronted with *Z. tritici* blastospores, no peak corresponding to the retention time and *m/z* 209.0455 $[M-H]^-$ of the authentic chemical standard of 2,4-DAPG was detected (Fig. 5c).

Discussion

Our approach utilised a novel high throughput phenotyping screening methodology to identify environmental *Pseudomonas* isolates with an ability to suppress growth of the wheat pathogen *Z. tritici* in vitro. We combined an in vitro phenotyping method with genome mining of antagonistic *Pseudomonas* isolates to identify putative antifungal secondary metabolite biosynthetic gene clusters and associated gene cluster families. This led to the identification of 52 isolates from a collection of 534 with an ability to suppress *Z. tritici* IPO323 blastospores in vitro. Genome sequencing and assembly of a subset of this collection, comprising 5 antagonistic and 6 non-antagonistic strains was conducted, followed by the prediction of 131 BGCs that formed 46 discrete GCF networks.

In addition to demonstrating high throughput qualitative screening, our results also indicate that the blastospore antagonism assay can be used to quantitatively assess antagonism of *Z. tritici* growth by *Pseudomonas* isolates in vitro, albeit with lower throughput due to increased spacing of bacterial cultures on test plates and the requirement to adopt digital image analysis to quantify inhibition zones. We believe that this assay can be expanded to assess the ability of other microbial species to suppress *Z. tritici* growth, though we recommend that this is not done in a disparate manner (e.g., wholesale screening of bacterial culture collections), but rather tailored toward specific bacterial genera to reduce the likelihood of potential quality control issues when simultaneously screening bacteria with inherently different growth kinetics.

Assessment of fungal antagonism by bacterial isolates is commonly conducted qualitatively, owing to the difficulty in quantifying antagonism of hyphal networks growing across entire plates in vitro. A high throughput semi-solid medium based screen has been described, using spectrophotometer measurements (OD_{600}) and turbidimetric measurements to quantify growth of the pathogenic fungus *Aspergillus flavus* when exposed to chemical libraries, to screen for antagonism of the fungus through a reduction in growth rate compared to control[30]. However, the application of this technique is limited for our purposes, due to the overlapping spectra commonly used to quantify the growth of bacteria and *Z. tritici*, hampering the discrimination of bacterial isolates and *Z. tritici* growth.

We report the first study to find significant differences in the response of genetically diverse isolates of *Z. tritici* to bacterial antagonists. Our ability to identify subtle differences in the in vitro growth profiles of *Z. tritici* in a quantitative manner, when confronted with a given antagonistic pseudomonad, indicates that natural variation in sensitivity or resistance to bacterial antagonists and associated secondary metabolites exists amongst *Z. tritici* isolates obtained from across Europe. We found that significant differences in the variability of inhibition between the original *Z. tritici* reference isolate IPO323 (isolated in 1984) and the more recently isolated strains were observed in response to confrontation with some pseudomonads, such as BFR20. This suggests that selection for broad spectrum antifungal insensitivity in *Z. tritici* across this period, may be correlated with differences in response to in vitro bacterial antagonism and further studies to identify mechanistic understanding of this phenomenon are required.

A number of quantitative traits have been identified in *Z. tritici* populations, such as temperature tolerance[31], and fungicide resistance[32]. The results presented within this study highlight the possibility that sensitivity to bacterial antagonism may also exist as a quantitative trait within natural *Z. tritici* populations. The patterns of sensitivity of *Z. tritici* isolates to antagonism by *Pseudomonas* isolates show that no *Z. tritici* isolate tested was consistently the most sensitive or resistant towards all antagonistic *Pseudomonas* isolates screened. Our antagonism phenotype paired bioinformatic analyses suggest that this could indicate differing underlying mechanisms of antagonism by the *Pseudomonas* isolates and potentially differing genetic targets for antagonism in *Z. tritici* blastospores, or differing levels of tolerance to antifungal metabolites in the *Z. tritici* test set. Differences in *Z. tritici* genotype-specific sensitivity to 2,4-DAPG could reflect variation in tolerance mechanisms such as metabolic detoxification as previously proposed for tolerant *Fusarium oxysporum* isolates[33], although this was not investigated within this study. In future work it will be interesting to generate mapping populations of sexual crosses between *Z. tritici* isolates resistant and/or sensitive to particular bacterial antagonists, to identify possible 'modes-of-action' of bacterial antagonists. This could be achieved through the screening of the mapping population in the blastospore confrontation assay, and the use of genome-wide association study (GWAS) approaches to identify genomic regions in *Z. tritici* associated with heightened sensitivity or resistance to antagonism.

A limitation of our described approach is that the observed zones of clearing produced by antagonistic *Pseudomonas* isolates are potentially constrained by the diffusion of secreted compounds involved in antagonism through the agar medium. This could limit the ability of this screen to identify subtle changes in sensitivity of *Z. tritici* isolates to classes of secreted high-molecular weight compounds such as lipopeptides[34–36] in a high throughput manner. However, lower throughput microscopic image analysis to assess fungal blastospore density in response to confrontation will facilitate the determination of infraspecific suppressive activity of pseudomonads. A further limitation is that in vitro antagonism does not necessarily translate to *in planta* efficacy, where compound stability and diffusion alongside many biotic and abiotic factors, can strongly influence outcomes, as previous studies have shown[37]. The validation of candidate metabolites for antifungal activity against *Z. tritici in* agronomically relevant scenarios represents an important next step outside the scope of the present proof-of-concept study.

The 11 *Pseudomonas* isolates screened for antagonism of genetically diverse *Z. tritici* isolates were analysed bioinformatically to obtain predictions of secondary metabolite BGCs from genome assemblies. This analysis indicated that known antifungal secondary metabolite BGCs, such as genes for 2,4-DAPG production, were implicated in fungal suppression in vitro. However, we also found that for *P. mandelii* subgroup isolate BFB20,

a mechanism of antagonism through the production of known secreted antifungal secondary metabolites could not be inferred from predicted BGC similarity to MIBiG reference BGCs. Additionally, the genome assembly of *P. mandelii* isolate BFR20 only contained one predicted BGC found to be significantly similar to the MiBIG reference BGC for Pf-5 pyoverdine (BGC0000413), though BGCs in this GCF were also predicted from non-antagonistic strains Roth17, Roth40, Roth97, and Roth105. The observed antagonism phenotype of these strains, BFB20 and BFR20, could therefore be due to the production of potentially novel secondary metabolites, encoded by BGCs dissimilar to reference BGCs from the MIBiG repository. As such these strains, and predicted BGCs within GCFs deriving solely from antagonistic isolates, namely GCF_00030, GCF_00023, and GCF_00028 (all predicted from BFR20), GCF_02559 (predicted from BFR20 and Roth112), and GCF_00016 (predicted from BFB20), should be prioritised in future work for further characterisation and the potential discovery of new antifungal molecules. These findings are consistent with previous studies that found many predicted secondary metabolite BGCs from *Pseudomonas* type strains were significantly dissimilar to known reference BGCs from the MiBIG repository, and therefore potentially encode novel secondary metabolites[9]. Characterisation of predicted BGCs with significant similarity to reference BGCs encoding 2,4-DAPG production in isolates Roth107 and Roth112 (*P. corrugata* subgroup) will determine whether the observed in vitro antagonism phenotype is solely due to 2,4-DAPG production, or if other predicted BGCs encoding unknown secondary metabolite products contribute to the phenotype. Notably, Roth112 showed consistently stronger antagonism than Roth82 against *Z. tritici* isolates in vitro (Fig. 2), which may reflect increased 2,4-DAPG contribution and/or additional bioactive metabolites acting alongside 2,4-DAPG. Roth112 is therefore a priority target for future functional characterisation to dissect the basis of this phenotype. However, our results showed that the in vitro antagonism of isolate Roth82 (*P. corrugata* subgroup) appeared to be solely due to 2,4-DAPG production.

Three antagonistic bacteria were bioinformatically predicted to have the potential to biosynthesise the antifungal polyketide 2,4-DAPG. Production of 2,4-DAPG has been described from two *Pseudomonas* species subgroups, *P. corrugata* and *P. protegens*[38–42], and more recently in the genus *Chromobacterium*[43]. This corroborates with the putative classification of Roth82, and Roth107, and Roth112 as within the *P. corrugata* subgroup based on taxonomic inference within this study, and the presence of a predicted BGC with high sequence similarity to 2,4-DAPG reference BGCs[38,26,41,42]. Predicted BGCs with a high sequence similarity to those encoding the biosynthesis of pyoverdines[44] and pseudomonine[45] were also predicted from the genome assemblies of *Pseudomonas* isolates within this study but were either found in an equal number of *Z. tritici* antagonistic and non-antagonistic strains (pyoverdine), or solely from *Z. tritici* non-antagonistic isolates (pseudomonine). Whilst these BGCs were not taken forward for further characterisation in respect to the *Z. tritici* antagonism phenotype, it is possible that diversity in the expression profiles of these BGCs exist between the *Pseudomonas* isolates, or that the siderophore products of these BGCs differ between isolates. For this reason, predicted BGC presence/absence was only used to enable prioritisation of BGCs associated with *Z. tritici* antagonism phenotypes, rather than provide definitive identifications of similarity. Whilst these predicted BGCs did not appear to be strongly associated with the *Z. tritici* blastospore antagonism phenotype, they could be implicated in antagonistic interactions with other fungi, or with *Z. tritici* under different environmental conditions or contexts. For example, differing carbon sources have previously been shown to influence 2,4-DAPG production by *Pseudomonas* strain F113[46]. This highlights a strength of a phenotype-guided genome mining for secondary metabolites involved in microbial interactions within simplified experimental contexts.

As a proof of concept, we generated a 2,4-DAPG insertional mutant, by disrupting the core gene encoding the biosynthetic enzyme PhlD. This enzyme is responsible for the production of monoacetylphloroglucinol (MAPG), that undergoes subsequent acetylation to produce 2,4-DAPG[26]. This resulted in no detectable production of 2,4-DAPG in Roth82 *phlD*::pKNOCK-Km, and a loss of the visible zone of inhibition in the *Z. tritici* blastospore antagonism assay, confirming the validity of our approach to determine mode of action of known antifungal BGCs. It will be interesting to use this approach to quantify the relative contribution of predicted secondary metabolite BGCs to the *Z. tritici* antagonism phenotype where multiple antifungal BGCs are predicted in a strain. For bacterial isolates where mechanisms of antagonism cannot be bioinformatically predicted, analytical chemistry of isolate extracts can facilitate the identification of molecules implicated in fungal suppression. This, when coupled with other approaches such as the creation and screening of transposon mutant libraries can facilitate the identification of previously unknown antifungal molecules. Similarly, the in vitro Z. tritici blastospore antagonism assay could be adapted to screen fractions and/or compounds of interest and could be used in a bioassay-guided fractionation approach.

The efficacy of biological control agents added to environmental settings is often unpredictable[47]. Our approach of identifying molecules responsible for the suppression of *Z. tritici* does not rely on phyllosphere competence and/or production of antifungal secondary metabolites in situ on the plant surface. The method described can be used to efficiently and cost-effectively mine bacterial strain collections for novel antifungal secondary metabolites that are effective against *Z. tritici* in an in vitro setting. Furthermore, the described *Pseudomonas-Zymoseptoria* interaction system could be further exploited as a potential 'stepping-stone' for the identification of broad spectrum antifungal secondary metabolites with activity against other fungal plant pathogens, that are less amenable to high-throughput in vitro screening, as well as medically important fungi such as *Candida* and *Aspergillus* spp.

Methods

Pseudomonas isolate collection

The library of 534 *Pseudomonas* wheat root associated isolates utilised in this study were generated previously at Rothamsted Research in Harpenden, UK[20,48] and maintained as glycerol stocks in the Rothamsted microbial culture collection at -80 °C.

Zymoseptoria tritici isolate collection

Twelve genetically diverse *Z. tritici* isolates utilised in this study were isolated from across Europe in 2016 as part of a previous study[23], with the exception of *Z. tritici* isolate IPO323, the reference strain first isolated in the Netherlands in 1984[49].

Culturing of Pseudomonads and *Z. tritici*

Zymoseptoria tritici blastospores were cultured by spreading 30 µl of defrosted glycerol stock on potato dextrose agar (PDA, Formedium) plates, before inverting and placing in darkness at 16 °C for 5 days. Blastospores were harvested using a sterile loop after 5 days of growth. *Pseudomonas* isolates were cultured from glycerol stocks, by inoculating 10 ml of LB Miller Broth (Formedium), with a chip (approximately 5 µl volume) of frozen glycerol stock. The inoculated broth was placed in a shaking incubator at 180 rpm and 25 °C overnight (18 h).

Zymoseptoria tritici blastospore antagonism assay

To qualitatively assess *Z. tritici* antagonism, a 20 µl loop of harvested *Z. tritici* blastospores was vortexed with 5 ml of distilled water, resulting in the formation of a suspension of approximately 1×10^6 blastospores per ml[23]. Next, 800 µl of spore suspension was added to a 120 mm x 120 mm Petri dish plates containing 50 ml PDA (Formedium). Plates were tilted to ensure a confluent inoculation of the blastospore suspension across the entire plate before excess spore suspension was recovered. Plates were air-dried for 20 min in a laminar flow hood, before 1 µl of 0.6 OD_{600} of a given *Pseudomonas* overnight culture was applied. A total of up to 48 *Pseudomonas* isolates were arrayed per plate in triplicate. Plates were sealed with Parafilm (Amcor) and inverted, before incubation in darkness at 16 °C for 12 days, prior to assessment for fungal growth inhibition. Images were taken after 12 days from a standardised height of 78.5 cm, using a Nikon D80 digital camera with a Sigma 70 mm F2.8 DG Macro lens (settings ISO 400, RAW image quality, large image size).

When performing quantitative antagonism measurements, the assay was conducted as described above with increased spacing; 11 *Pseudomonas* isolates and an overnight LB Miller Broth (Formedium) negative control were included per plate and four replicate plates were prepared in a factorial design. Images of confrontation plates were used to measure fungal growth inhibition as described above. Measurements were taken from the edge of the bacterial colony to the outer boundary of the visible zone of clearing of *Z. tritici* blastospores, in a radial manner from the centre of the bacterial colony, using FIJI/ImageJ (version 2.1.0/1.53c) to quantify the number of pixels (2253 pixels = 1 mm). For each bacterial colony, three independent radial measurements were taken using a randomly generated measurement angle (1–360°) from the colony centre. Where a randomly selected radial intersected a region in which zones of clearing from neighbouring colonies met or overlapped, such that the boundary could not be unambiguously attributed to a single colony, that direction was treated as non-measurable and a new random angle was generated. Figures 1a and 2a were created using BioRender.

Genome sequencing of *Pseudomonas* isolates

Genome sequencing was provided by MicrobesNG (http://www.microbesng.com). Draft genome assemblies for 11 *Pseudomonas* isolates were generated using 250 bp paired end Illumina MiSeq. Sequences were passed through their bioinformatic pipeline consisting of Kraken[50], BWA mem[51], before genomes were assembled *de novo* using SPAdes[52] and annotated using Prodigal[53].

BUSCO (Benchmarking Universal Single-Copy Orthologs) analysis

BUSCO analysis of genomes was carried out on a local server using BUSCO version 5.2.2[54], using the bacterial odb10 reference single copy orthologous genes dataset for bacterial species to assess genome assemblies for bacterial contamination, and the Pseudomonadales odb10 reference dataset to assess genome assembly completeness.

Phylogenetic tree construction

A phylogenetic tree was constructed using Automated Multi-Locus Species Tree (autoMLST), based on a concatenation of 100 common genes (Table S3) found across the genome assemblies of the 11 *Pseudomonas* isolates within this study, and the closest 50 reference genome assemblies from RefSeq[27]. Annotations to the phylogenetic tree were added using ITOL[55]. Clades within the phylogenetic tree were annotated, to indicate the *Pseudomonas* subgroups present as defined by[28]. Type strain *Pseudomonas* genomes were identified using The List of Prokaryotic names with Standing in Nomenclature (LPSN) (https://lpsn.dsmz.de/) accessed on the 24th January 2025.

Secondary metabolite biosynthetic gene cluster prediction and sequence similarity network (SSN) generation

Secondary metabolite biosynthetic gene clusters were predicted using antiSMASH 7.0.0 on a local server for 5 antagonistic and 6 non-antagonistic *Pseudomonas* genome sequences. Sequence similarity networks (SSN) were constructed from the antiSMASH 7.0.0 output from the 11 antagonistic *Pseudomonas* genome sequences, using BiG-SCAPE version 1.1.5[25] and Pfam 35[56] on a local server. A cut-off value of 0.3 was used, and 1,808 reference sequences from the MIBiG database were included in the construction of Gene Cluster Family (GCF) networks based on sequence similarity, with visualisations of SSNs generated and edited in Cytoscape 3.10.1[57]. Regions containing predicted BGCs that formed a SSN with MIBiG reference BGCs for 2,4-diacetylphloroglucinol (BGC0000280 & BGC0000281) were aligned using clinker version 0.0.23[58], before trimming to remove sequence upstream and downstream of the predicted BGCs. Colour schemes of plots were modified using Inkscape version 1.3 (Available from: https://inkscape.org).

Construction of *phlD* insertional mutant

To generate Roth82 *phlD*::pKNOCK-Km an internal fragment (333 bp) of the *phlD* gene was amplified by PCR using primers (pKNOCK*PhlD*3_Fw: GTCGGATCCACATCGTGCACCGGTTTCAT and pKNOCK*PhlD*3_Rv: GTCGGTACCGTAAGACCCGGTATTGGCG), verified by DNA sequencing and cloned as a *Bam*HI-*Kpn*I fragment into corresponding sites of pKNOCK-Km[59], resulting in pKNOCK*phlD*. Electrocompetent Roth82 cells were prepared as described by Choi et al.,[60]. We added 300 ng of pKNOCK*phlD* DNA to the prepared electrocompetent cells and transferred to a pre-chilled 2 mm gap electroporation cuvette. The plasmid construct was delivered to electrocompetent *Pseudomonas* isolate Roth82 by electroporation (2.5 kV, 25 µF and 200 Ω). Immediately following electroporation, 1 mL of LB was added and cells recovered at 25 °C with 200 rpm shaking for 1 h, before plating. Transformants were then selected by plating 100 µL of the recovery culture on LB agar supplemented with kanamycin (50 µg/mL), before incubation at 25 °C for 18 h. Single colonies of putative transformants were purified on LB agar supplemented with kanamycin (50 µg/mL) prior to PCR confirmation. The mutant Roth82 *phlD*::pKNOCK-Km was confirmed by colony PCR using external primers flanking the insertion region (pKnockPhlD2_Fw: ATGATGCCCTCGCTGAC, pKnockPhlD2_Rv: CCGGGTTCCAAGTC CAGT, pKNOCKcheckFw: GGACAACAAGCCAGGGATGTA and pKNOCKcheckRv: ATGTAAGCCCACTG CAAGCTA), resulting in the expected size shift (wild-type 527 bp; mutant 2098 bp, Figure S6), and by Sanger sequencing at Eurofins (Germany).

Chemical extraction of secondary metabolites from *Z. tritici* antagonism assay

A 10 mm diameter section of agar surrounding the *Pseudomonas* colony edge was excised from wild-type Roth82 and mutant Roth82 *phlD*::pKNOCK-Km grown with and without *Z. tritici* confrontation on PDA plates. Chemical extracts were prepared by macerating agar sections in 1 ml HPLC grade MeOH, with resulting solutions centrifuged at > 13,000 rpm for 10 min. Supernatant was collected for analysis by liquid chromatography-mass spectrometry (LC-MS).

Chemical analysis of secreted secondary metabolites produced by *Pseudomonas* isolates

UPLC was conducted on agar extracts using an ACQUITY UPLC® system equipped with an ACQUITY BEH C18 (1.7 µm, 2.1 × 50 mm) analytical column (Waters, USA). Extracts were eluted over 38 min from 5% to 95% organic (UPLC grade water + 0.1% formic acid and MeOH + 0.1% formic acid) at a flow rate of 0.21 mL min^{-1}. The UPLC system was coupled with quadrupole time-of-flight mass spectrometer SYNAPT G2-Si (Waters, USA), with electrospray ion source run in negative and positive ionisation mode and data acquired over 50–1200 m/z range. The lock mass solution consisted of Leucine Enkephalin (200 pg/µL). The lockspray was acquired during UPLC-MS acquisition and corrected for ($[M + H]^+$ m/z 556.2771 & $[M-H]^-$ m/z 554.2615). Instrument control and data acquisition was carried out in MassLynx (Waters, USA). Data was converted to mzML format using Waters2mzML V1.2.0 (available at https://github.com/AnP311/Waters2mzML), before Extracted Ion Chromatograms (EICs) were generated using mzmine 4.3.0[61].

Statistical analyses

Analysis of Variance (ANOVA) was used to determine significant differences in the size of zones of inhibition. Zone of inhibition data of *Z. tritici* isolates in confrontation with *Pseudomonas* isolate BFR20 were log transformed, to fulfil the requirement of analysis of variance (ANOVA) for data to be approximately normally distributed. Zone of inhibition data for all other antagonistic *Pseudomonas* isolates were found to be approximately normally distributed without transformation. Sidak's multiple comparison post-hoc test was used to examine pairwise data comparisons between *Z. tritici* genotypes at the 5% level of significance. All statistical analyses were carried out in RStudio (2023.03.0 Build 386, R version 4.2.3), using packages ggplot2 (3.4.4)[62], dplyr (1.1.4)[63], ggpubr (0.6.0)[64], emmeans (1.10.0)[65], multcomp (1.4–25)[66] and svglite (2.1.3)[67].

Data availability

The *Pseudomonas* genome assemblies are publicly available in NCBI Bioproject: PRJNA1164014, BioSamples SAMN55848972-SAMN55848982. Raw data associated with this publication is available at https://doi.org/10.23637/wya4d1b7, scripts associated with analysis of data available at https://github.com/iamgeorgelund/PseudomonasZymoseptoria and mirrored in a permanent Zenodo repository at https://doi.org/10.5281/zenodo.18865490. The *Pseudomonas* isolate collection and *Zymoseptoria tritici* isolate collection used in this study are available to academic researchers for non-commercial research purposes upon reasonable request to the corresponding author and will be provided under a standard institutional material transfer agreement (MTA) to document transfer and ensure compliance with biosafety and shipping requirements.

Received: 18 June 2025; Accepted: 6 April 2026
Published online: 02 May 2026

References

1. Torriani, S. F. F. *Zymoseptoria tritici*: A major threat to wheat production, integrated approaches to control. *Fungal Genet. Biol.* **5**. (2015).
2. Lucas, J. A., Hawkins, N. J. & Fraaije, B. A. The Evolution of Fungicide Resistance, in: Advances in Applied Microbiology. Elsevier, 29–92. https://doi.org/10.1016/bs.aambs.2014.09.001 (2015).
3. Barka, E. A. et al. Taxonomy, Physiology, and Natural Products of Actinobacteria. *Microbiol. Mol. Biol. Rev.* **80**, 1–43. https://doi.org/10.1128/MMBR.00019-15 (2016).
4. Kerr, K. G. & Snelling, A. M. *Pseudomonas aeruginosa*: a formidable and ever-present adversary. *J. Hosp. Infect.* **73**, 338–344. https://doi.org/10.1016/j.jhin.2009.04.020 (2009).

5. Morris, C. E., Monteil, C. L. & Berge, O. The Life History of *Pseudomonas syringae*: Linking Agriculture to Earth System Processes. *Annu. Rev. Phytopathol.* **51**, 85–104. https://doi.org/10.1146/annurev-phyto-082712-102402 (2013).
6. Santoyo, G. Plant growth-promoting bacterial endophytes. *Microbiol. Res.* **8**. (2016).
7. Höfte, M. in *The use of Pseudomonas spp. as bacterial biocontrol agents to control plant diseases*. Burleigh Dodds Series in Agricultural Science301–374 (eds University, W., Research & Köhl, J.) (Burleigh Dodds Science Publishing, 2021). https://doi.org/10.19103/AS.2021.0093.11
8. Thomashow, L. S. & Weller, D. M. Current Concepts in the Use of Introduced Bacteria for Biological Disease Control: Mechanisms and Antifungal Metabolites, in: (eds Stacey, G. & Keen, N. T.) Plant-Microbe Interactions. Springer US, Boston, MA, 187–235. https://doi.org/10.1007/978-1-4613-1213-0_6 (1996).
9. Saati-Santamaría, Z., Selem-Mojica, N., Peral-Aranega, E., Rivas, R. & García-Fraile, P. Unveiling the genomic potential of *Pseudomonas* type strains for discovering new natural products. *Microb. Genomics*. **8** https://doi.org/10.1099/mgen.0.000758 (2022).
10. Flaishman, M., Eyal, Z., Voisard, C. & Haas, D. Suppression ofSeptoria tritici by Phenazine- or Siderophore-deficient mutants ofPseudomonas. *Curr. Microbiol.* **20**, 121–124. https://doi.org/10.1007/BF02092884 (1990).
11. Levy, E., Eyal, Z., Carmely, S., Kashman, Y. & Chet, I. Suppression of Septoria tritici and Puccinia recondita of wheat by an antibiotic-producing fluorescent pseudomonad. *Plant. Pathol.* **38**, 564–570. https://doi.org/10.1111/j.1365-3059.1989.tb01452.x (1989).
12. Levy, E., Eyal, Z., Chet, I. & Hochman, A. Resistance mechanisms of Septoria tritici to antifungal products of Pseudomonas. *Physiol. Mol. Plant Pathol.* **40**, 163–171. https://doi.org/10.1016/0885-5765(92)90057-3 (1992a).
13. Levy, E., Gough, F. J., Berlin, K. D., Guiana, P. W. & Smith, J. T. Inhibition of Septoria tritici and other phytopathogenic fungi and bacteria by Pseudomonas fluorescens and its antibiotics. *Plant. Pathol.* **41**, 335–341. https://doi.org/10.1111/j.1365-3059.1992.tb02355.x (1992b).
14. Levy, E., Eyal, Z. & Chet, I. Suppression of septoria tritici blotch and leaf rust on wheat seedling leaves by pseudomonads. *Plant. Pathol.* **37**, 551–557. https://doi.org/10.1111/j.1365-3059.1988.tb02114.x (1988).
15. Lindberg, G. D., Larkin, J. M. & Whaley, H. A. Production of Tropolone by A Pseudomonas. *J. Nat. Prod.* **43**, 592–594. https://doi.org/10.1021/np50011a011 (1980).
16. Flaishman, M. A. Suppression of Septoria tritici Blotch and Leaf Rust of Wheat by Recombinant Cyanide-Producing Strains of *Pseudomonas putida*. *MPMI* **9**, 642. https://doi.org/10.1094/MPMI-9-0642 (1996).
17. Chen, R. S. & McDonald, B. A. Sexual Reproduction Plays a Major Role in the Genetic Structure of Populations of the Fungus *Mycosphaerella graminicola*. *Genetics* **142**, 1119–1127. https://doi.org/10.1093/genetics/142.4.1119 (1996).
18. Linde, C. C., Zhan, J. & McDonald, B. A. Population Structure of Mycosphaerella graminicola: From Lesions to Continents. *Phytopathology*® **92**, 946–955. https://doi.org/10.1094/PHYTO.2002.92.9.946 (2002).
19. Bubici, G., Kaushal, M., Prigigallo, M. I., Gómez-Lama Cabanás, C. & Mercado-Blanco, J. Biological Control Agents Against Fusarium Wilt of Banana. *Front. Microbiol.* **10**, 616. https://doi.org/10.3389/fmicb.2019.00616 (2019).
20. Mauchline, T. H. et al. An analysis of *Pseudomonas* genomic diversity in take-all infected wheat fields reveals the lasting impact of wheat cultivars on the soil microbiota. *Environ. Microbiol.* **17**, 4764–4778. https://doi.org/10.1111/1462-2920.13038 (2015).
21. Gross, H. & Loper, J. E. Genomics of secondary metabolite production by Pseudomonas spp. *Nat. Prod. Rep.* **26**, 1408. https://doi.org/10.1039/b817075b (2009).
22. Terlouw, B. R. et al. MIBiG 3.0: a community-driven effort to annotate experimentally validated biosynthetic gene clusters. Nucleic Acids Research 51, D603–D610. (2023). https://doi.org/10.1093/nar/gkac1049
23. Chen, H. et al. Combined pangenomics and transcriptomics reveals core and redundant virulence processes in a rapidly evolving fungal plant pathogen. *BMC Biol.* **21**, 24. https://doi.org/10.1186/s12915-023-01520-6 (2023).
24. Blin, K. et al. antiSMASH 7.0: new and improved predictions for detection, regulation, chemical structures and visualisation. *Nucleic Acids Res.* **51**, W46–W50. https://doi.org/10.1093/nar/gkad344 (2023).
25. Navarro-Muñoz, J. C. et al. A computational framework to explore large-scale biosynthetic diversity. *Nat. Chem. Biol.* **16**, 60–68. https://doi.org/10.1038/s41589-019-0400-9 (2020).
26. Bangera, M. G. & Thomashow, L. S. Identification and Characterization of a Gene Cluster for Synthesis of the Polyketide Antibiotic 2,4-Diacetylphloroglucinol from *Pseudomonas fluorescens* Q2-87. *J. Bacteriol.* **181**, 3155–3163. https://doi.org/10.1128/JB.181.10.3155-3163.1999 (1999).
27. Alanjary, M., Steinke, K. & Ziemert, N. AutoMLST: an automated web server for generating multi-locus species trees highlighting natural product potential. *Nucleic Acids Res.* **47**, W276–W282. https://doi.org/10.1093/nar/gkz282 (2019).
28. Hesse, C. et al. Genome-based evolutionary history of *Pseudomonas* spp. *Environ. Microbiol.* **20**, 2142–2159. https://doi.org/10.1111/1462-2920.14130 (2018).
29. Lauritsen, J. G. et al. Identification and Differentiation of *Pseudomonas* Species in Field Samples Using an rpoD. *Amplicon Sequencing Methodol.* **6**, 14 (2021).
30. Medina, A., Lambert, R. J. W. & Magan, N. Rapid throughput analysis of filamentous fungal growth using turbidimetric measurements with the Bioscreen C: a tool for screening antifungal compounds. *Fungal Biology*. **116**, 161–169. https://doi.org/10.1016/j.funbio.2011.11.001 (2012).
31. Lendenmann, M. H., Croll, D., Palma-Guerrero, J., Stewart, E. L. & McDonald, B. A. QTL mapping of temperature sensitivity reveals candidate genes for thermal adaptation and growth morphology in the plant pathogenic fungus Zymoseptoria tritici. *Heredity* **116**, 384–394. https://doi.org/10.1038/hdy.2015.111 (2016).
32. Lendenmann, M. H., Croll, D. & McDonald, B. A. QTL mapping of fungicide sensitivity reveals novel genes and pleiotropy with melanization in the pathogen Zymoseptoria tritici. *Fungal Genet. Biol.* **80**, 53–67. https://doi.org/10.1016/j.fgb.2015.05.001 (2015).
33. Schouten, A. et al. Defense Responses of *Fusarium oxysporum* to 2,4-Diacetylphloroglucinol, a Broad-Spectrum Antibiotic Produced by *Pseudomonas fluorescens*. *MPMI* **17**, 1201–1211. https://doi.org/10.1094/MPMI.2004.17.11.1201 (2004).
34. Berry, C. Lipopeptides are essential for Pseudomonas sp. DF41 biocontrol of Sclerotinia sclerotiorum. *Biol. Control* **9**. (2010).
35. Geudens, N. & Martins, J. C. Cyclic Lipodepsipeptides From Pseudomonas spp. – Biological Swiss-Army Knives. *Front. Microbiol.* **9**, 1867. https://doi.org/10.3389/fmicb.2018.01867 (2018).
36. Mejri, S. et al. Biocontrol of the wheat pathogen Zymoseptoria tritici using cyclic lipopeptides from Bacillus subtilis. *Environ. Sci. Pollut Res.* **25**, 29822–29833. https://doi.org/10.1007/s11356-017-9241-9 (2018).
37. Kildea, S. et al. Bacillus megaterium shows potential for the biocontrol of septoria tritici blotch of wheat. *Biol. Control* **9**. (2008).
38. Abbas, A. et al. Characterization of Interactions between the Transcriptional Repressor PhlF and Its Binding Site at the *phlA* Promoter in *Pseudomonas fluorescens* F113. *J. Bacteriol.* **184**, 3008–3016. https://doi.org/10.1128/JB.184.11.3008-3016.2002 (2002).
39. Almario, J. et al. Distribution of 2,4-Diacetylphloroglucinol Biosynthetic Genes among the Pseudomonas spp. *Reveals Unexpected Polyphyletism Front. Microbiol.* **8**, 1218. https://doi.org/10.3389/fmicb.2017.01218 (2017).
40. Frapolli, M., Défago, G. & Moënne-Loccoz, Y. Multilocus sequence analysis of biocontrol fluorescent *Pseudomonas* spp. producing the antifungal compound 2,4-diacetylphloroglucinol. *Environ. Microbiol.* **9**, 1939–1955. https://doi.org/10.1111/j.1462-2920.2007.01310.x (2007).
41. Hansen, M. L., He, Z., Wibowo, M. & Jelsbak, L. A Whole-Cell Biosensor for Detection of 2,4-Diacetylphloroglucinol (DAPG)-Producing Bacteria from Grassland Soil. *Appl. Environ. Microbiol.* **87**, e01400–e01420. https://doi.org/10.1128/AEM.01400-20 (2021).

42. Raaijmakers, J. M. & Weller, D. M. Natural Plant Protection by 2,4-Diacetylphloroglucinol-Producing *Pseudomonas* spp. *Take-All Decline Soils MPMI*. **11**, 144–152. https://doi.org/10.1094/MPMI.1998.11.2.144 (1998).
43. Johnson, E. T., Bowman, M. J., Gomes, R. P., Carneiro, L. C. & Dunlap, C. A. Identification of 2,4-diacetylphloroglucinol production in the genus Chromobacterium. *Sci. Rep.* **13**, 14292. https://doi.org/10.1038/s41598-023-41277-0 (2023).
44. Hartney, S. L. et al. Ferric-Pyoverdine Recognition by Fpv Outer Membrane Proteins of Pseudomonas protegens Pf-5. *J. Bacteriol.* **195**, 765–776. https://doi.org/10.1128/JB.01639-12 (2013).
45. Mercado-Blanco, J. et al. Analysis of the pmsCEAB gene cluster involved in biosynthesis of salicylic acid and the siderophore pseudomonine in the biocontrol strain Pseudomonas fluorescens WCS374. *J. Bacteriol.* **183**, 1909–1920. https://doi.org/10.1128/JB.183.6.1909-1920.2001 (2001).
46. Shanahan, P., O'Sullivan, D. J., Simpson, P., Glennon, J. D. & O'Gara, F. Isolation of 2,4-Diacetylphloroglucinol from a Fluorescent Pseudomonad and Investigation of Physiological Parameters Influencing Its Production. *Appl. Environ. Microbiol.* **58**, 353–358. https://doi.org/10.1128/AEM.58.1.353-358.1992 (1992).
47. Collinge, D. B. et al. Biological control of plant diseases – What has been achieved and what is the direction? *Plant. Pathol.* **71**, 1024–1047. https://doi.org/10.1111/ppa.13555 (2022).
48. Ruscoe, H. L. et al. Land Management Legacy Affects Abundance and Function of the acdS Gene in Wheat Root Associated Pseudomonads. *Front. Microbiol.* **12**, 611339. https://doi.org/10.3389/fmicb.2021.611339 (2021).
49. Kema, G. H. J. & Van Silfhout, C. H. Genetic Variation for Virulence and Resistance in the Wheat- *Mycosphaerella graminicola* Pathosystem III. *Comp. Seedl. Adult Plant. Experiments Phytopathology*[*]. **87**, 266–272. https://doi.org/10.1094/PHYTO.1997.87.3.266 (1997).
50. Wood, D. E. & Salzberg, S. L. Kraken: ultrafast metagenomic sequence classification using exact alignments. *Genome Biol.* **15**, R46. https://doi.org/10.1186/gb-2014-15-3-r46 (2014).
51. Li, H. *Aligning sequence reads* (clone sequences and assembly contigs with BWA-MEM, 2013).
52. Prjibelski, A., Antipov, D., Meleshko, D., Lapidus, A. & Korobeynikov, A. Using SPAdes De Novo Assembler. *CP Bioinf.* **70**, e102. https://doi.org/10.1002/cpbi.102 (2020).
53. Hyatt, D. et al. Prodigal: prokaryotic gene recognition and translation initiation site identification. *BMC Bioinform.* **11**, 119. https://doi.org/10.1186/1471-2105-11-119 (2010).
54. Manni, M., Berkeley, M. R., Seppey, M., Simão, F. A. & Zdobnov, E. M. BUSCO Update: Novel and Streamlined Workflows along with Broader and Deeper Phylogenetic Coverage for Scoring of Eukaryotic, Prokaryotic, and Viral Genomes. *Mol. Biol. Evol.* **38**, 4647–4654. https://doi.org/10.1093/molbev/msab199 (2021).
55. Letunic, I. & Bork, P. Interactive Tree Of Life (iTOL) v4: recent updates and new developments. *Nucleic Acids Res.* **47**, W256–W259. https://doi.org/10.1093/nar/gkz239 (2019).
56. Mistry, J. et al. Pfam: The protein families database in 2021. *Nucleic Acids Res.* **49**, D412–D419. https://doi.org/10.1093/nar/gkaa913 (2021).
57. Shannon, P. et al. Cytoscape: A Software Environment for Integrated Models of Biomolecular Interaction Networks. *Genome Res.* **13**, 2498–2504. https://doi.org/10.1101/gr.1239303 (2003).
58. Gilchrist, C. L. M. & Chooi, Y. H. clinker & clustermap.js: automatic generation of gene cluster comparison figures. *Bioinformatics* **37**, 2473–2475. https://doi.org/10.1093/bioinformatics/btab007 (2021).
59. Alexeyev, M. F. The pKNOCK Series of Broad-Host-Range Mobilizable Suicide Vectors for Gene Knockout and Targeted DNA Insertion into the Chromosome of Gram-Negative Bacteria. *BioTechniques* **26**, 824–828. https://doi.org/10.2144/99265bm05 (1999).
60. Choi, K. H., Kumar, A. & Schweizer, H. P. A 10-min method for preparation of highly electrocompetent Pseudomonas aeruginosa cells: Application for DNA fragment transfer between chromosomes and plasmid transformation. *J. Microbiol. Methods*. **64**, 391–397. https://doi.org/10.1016/j.mimet.2005.06.001 (2006).
61. Schmid, R. et al. Integrative analysis of multimodal mass spectrometry data in MZmine 3. *Nat. Biotechnol.* **41**, 447–449. https://doi.org/10.1038/s41587-023-01690-2 (2023).
62. Wickham, H. ggplot2: Elegant Graphics for Data Analysis, Use R! Springer-Verlag New York. (2016). https://doi.org/10.1007/978-3-319-24277-4
63. Wickham, H., François, R., Henry, L., Müller, K. & Vaughan, D. dplyr: A Grammar of Data Manipulation. (2023).
64. Kassambara, A. *ggpubr: ggplot2* (Based Publication Ready Plots, 2023).
65. Lenth, R. V. emmeans: Estimated Marginal Means, aka Least-Squares Means. (2024).
66. Hothorn, T., Bretz, F. & Westfall, P. Simultaneous Inference in General Parametric Models. *Biom. J.* **50**, 346–363 (2008).
67. Wickham, H. et al. svglite: An SVG Graphics Device. (2024).

Acknowledgements

The authors thank Dr Vittorio Tracanna and Prof Marnix Medema for providing bioinformatics training essential to this study during G.L.'s placement at Wageningen University, and Dr Mike Birkett for his insightful comments and suggestions on the manuscript.The authors acknowledge funding from UK Biotechnology and Biological Sciences Research Council (BBSRC) Nottingham-Rothamsted Doctoral Training Partnership (grant number BB/M008770/1), and the Lawes Agricultural Trust. Rothamsted Science Initiatives Catalyst Award scheme grant 'Microbial natural product discovery pipeline for next generation fungicides'. Rothamsted Research receives strategic funding from the Biotechnology and Biological Sciences Research Council of the United Kingdom. We acknowledge support from the Institute Strategic Programmes: Growing Health (BB/X010953/1; BBS/E/RH/230003A and BBS/E/RH/230003B) and Delivering Sustainable Wheat (BB/X011003/1 and BBS/E/RH/230001B), as well as previous Institute Strategic Programmes: Designing Future Wheat (BBS/E/C000I0250), Soil 2 Nutrition (BBS/E/C/000I0310), and Smart Crop Protection (SCP, BBS/OS/CP/000001), funded through BBSRC's Industry Strategy Challenge Fund.

Author contributions

G.L., J.R. and T.H.M. acquired funding. G.L., S.M., D.M.W., I.M.C., J.R. and T.H.M. contributed to conceptualisation. G.L., S.M., D.M.W., J.R. and T.H.M. designed the experiments (methodology). G.L., S.M. and D.M.W. collected the data (investigation). J.C. and D.H. provided resources. Bioinformatic and statistical analyses were performed by G.L.; chemoinformatic analyses were conducted by G.L. and D.M.W. (software; formal analysis). G.L. curated the data and produced all visualisations (data curation; visualisation). I.M.C., J.R. and T.H.M. supervised the project (supervision). Results were interpreted by G.L., I.M.C., J.R., D.M.W. and T.H.M. The manuscript was written by G.L. and T.H.M., and all authors edited and commented on the manuscript (writing – original draft; writing – review & editing).

Declarations

Competing interests
The authors declare no competing interests.

Additional information
Supplementary Information The online version contains supplementary material available at https://doi.org/10.1038/s41598-026-48020-5.

Correspondence and requests for materials should be addressed to G.L.

Reprints and permissions information is available at www.nature.com/reprints.

Publisher's note Springer Nature remains neutral with regard to jurisdictional claims in published maps and institutional affiliations.